

# First-Principles Investigation About Different Sequence of Stereochemical Activity and Birefringence in Antimony Halides

Lu Li, Yanyan Qian, Xudong Leng, Xiuhua Cui, Haiming Duan, Ming-Hsien Lee, Haibin Cao, and Qun Jing\*

Birefringent compounds play an indispensable role in modern optoelectronics and information communication. In this article, the electronic structures and birefringence of binary and ternary antimony halides are investigated using the first-principles method. The results show that the stereochemical activity of antimony cations in these compounds gradually decreases from CI to I, and the birefringence of these compounds gradually increases from CI to I. The degree of stereochemical activity of lone pairs is determined by the energy difference between the s-state of the cation and the p-state of the halogen, implying the revised model about stereochemical activity of lone-pairs in metal oxides is also appropriate for metal halides. The real-space atomic cutting and Born effective charges show that the antimony cations and halogen closer to Fermi level give main contribution to birefringence. And the occupied p-states of antimony and halogen atoms play an important role in determining the birefringence.

#### 1. Introduction

Nonlinear optical (NLO) materials are a kind of important photoelectric functional materials, which have important applications in laser communication, laser micro-nanometer industry, and other fields.<sup>[1–11]</sup> In recent decades, a series of nonlinear

L. Li, Y. Qian, X. Leng, X. Cui, H. Duan, Q. Jing Xinjiang Key Laboratory of Solid State Physics and Devices Xinjiang University 666 Shengli Road, Urumqi 830046, China

E-mail: qunjing@xju.edu.cn

L. Li, Y. Qian, X. Leng, X. Cui, H. Duan, Q. Jing School of Physical Science and Technology Xinjiang University 666 Shengli Road, Urumqi 830046, China

M.-H. Lee Deparent of Physics Tamkang University New Taipei City 25137, Taiwan

H. Cao Deparent of Physics College of Sciences Shihezi University Shihezi 832000, China

The ORCID identification number(s) for the author(s) of this article can be found under https://doi.org/10.1002/pssb.202100576.

DOI: 10.1002/pssb.202100576

optical materials with excellent optical properties have been designed and synthesized, such as  $\beta\text{-BaB}_2\text{O}_4$  (BBO),  $^{[12]}$  LiB $_3\text{O}_5$  (LBO),  $^{[13]}$  CsB $_3\text{O}_5$  (CBO),  $^{[14]}$  KBe $_2\text{BO}_3\text{F}_2$  (KBBF). It is well known that nonlinear optical materials with excellent performance should have large second-harmonic generation (SHG) coefficients and appropriate birefringence.  $^{[17-24]}$ 

During the past decades, various chromophores have been introduced to obtain excellent optical performance. The chromophores are anionic groups with conjugated  $\pi$  bonds, groups containing  $d^0/d^{10}$  cations, post-transition metal cations, and so on.  $^{[25]}$  The post-transition metal cations containing  $ns^2np^0$  lone pair electrons (such as  $Pb^{2+},\ Sn^{2+},\ Bi^{3+},\ Sb^{3+},\ etc.)$  are able to obtain enhanced birefringence, due to

the asymmetric lone pair electronic distribution. [ $^{126}$ ] For example, our group has calculated the birefringence of  $M_2B_5O_9Cl$  (M=Sr, Ba, Pb) using the first-principles method, and the results show that the birefringence of  $Pb_2B_5O_9Cl$  is greater than that of its isomorphic alkaline earth metal borate  $M_2B_5O_9Cl$  (M=Sr, Ba). Liu et al. pointed out that  $SbB_3O_6$  has a large birefringence value (0.290@546 nm).  $^{[28]}$  The carbonate material  $CsPbCO_3F$  (0.104@1064 nm) containing  $Pb^{2+}$  cations and  $CO_3$  groups owns good mechanical stability and thermal stability  $^{[29,30]}$  and relatively large birefringence.  $^{[31]}$ 

In addition to metal oxides, a variety of metal halides or metal oxyhalides have also been found as an important class of optical materials. [32–35] For example, the mixed oxyhalides  $Pb_{17}O_8Cl_{18}$ , [32]  $Pb_{18}O_8Cl_{15}I_5$ , [33]  $Pb_{13}O_6Cl_9Br_5$ , [34] are good mid-infrared NLO candidates. As for metal halides, Gong et al. reported a family of metal halides  $RbSbF_3Cl$  and  $CsSbF_3Cl^{[36]}$  containing two different halogens, and the first-principles investigations show that the  $CsSbF_3Cl$  compound owns relatively large birefringence. Recently, Guo et al. pointed out that  $\alpha$ - $SnF_2$  has a broad transparent range and brilliant birefringence, and the birefringence of  $\alpha$ - $SnF_2$ ,  $PbCl_2$ , and  $SbCl_3$  are 0.177, 0.046, and 0.172 (@546 nm), respectively. [35] Curiously, could the stereochemically active lone pair be found in these metal halides? And what's the dominant factor determining the lone pair electronic distribution and birefringence?

In this work, the electronic structure and optical properties of a series of metal halides  $ASbF_3Cl$  (A = K, Rb, Cs) and  $SbX_3$ 

1521391, 2022, 7, Downloaded from https://onlinelibrary.wiley.com/doi/10.1002/pssb.202100576 by National Taiwam Universitate, Wiley Online Library on [1907/2023]. See the Terms and Conditions (https://onlinelibrary.wiley.com/terms-and-conditions) on Wiley Online Library for rules of use; OA articles are governed by the applicable Creative Commons Licenses

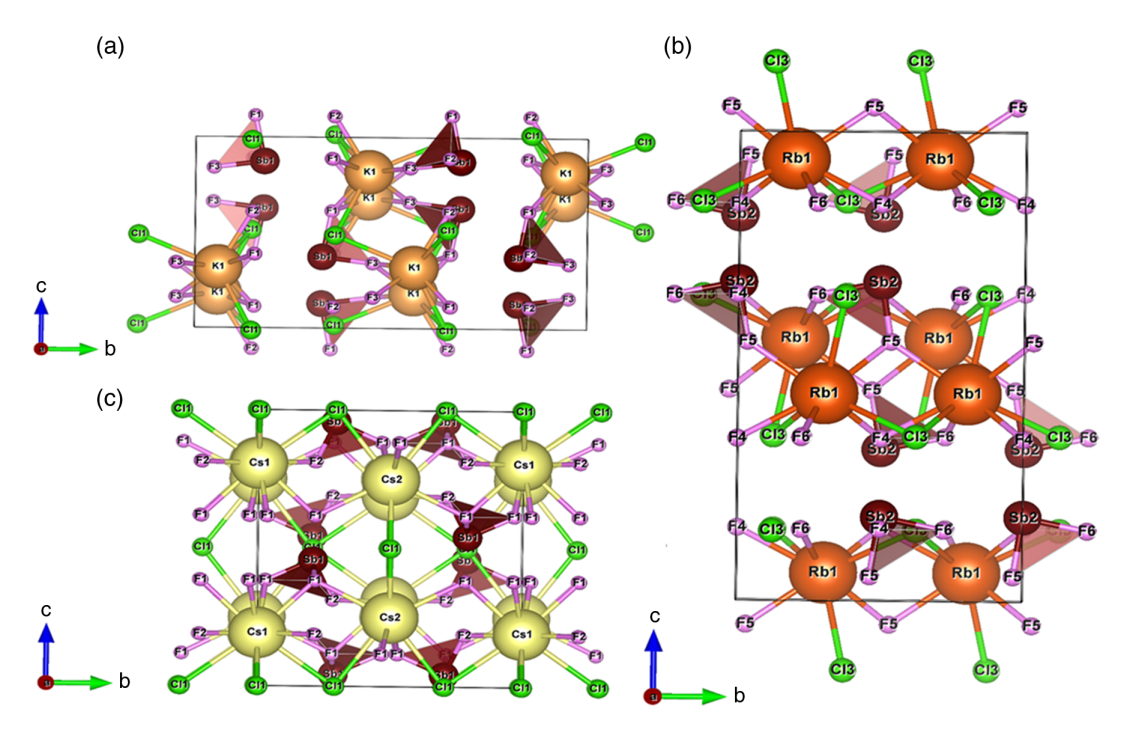


Figure 1. Crystal structures of: a) KSbF<sub>3</sub>Cl, b) RbSbF<sub>3</sub>Cl, and c) CsSbF<sub>3</sub>Cl.

(X = Cl, Br, I) are investigated using the first-principles method. The asymmetric lone pair electronic distribution is confirmed by the electronic orbitals nearby the Fermi level and electron localization function (ELF). The atomic contribution to birefringence is investigated using the real-space atomic cutting (RSAC) and Born effective charge. The results show that the stereochemical activity of antimony cations in these compounds gradually decreased from Cl to I, and the birefringence of these compounds gradually increased from Cl to I. The energy difference between s-states of antimony and p-states of halogen determines the stereochemical activity of lone pair electronic distribution. The energy difference between p states of antimony and halogen owns the sequence as Sb-Cl > Sb-Br > Sb-I, which determines the bandgap of metal halides. And the occupied p states of antimony and halogen atoms play an important role in determining the birefringence.

#### 2. Numerical Calculation Details

In this work, the CASTEP package,  $^{[37,38]}$  a plane-wave pseudopotential code based on the density functional theory (DFT),  $^{[39,40]}$  was used to investigate the electronic structures and optical properties. The geometry optimization was performed, and the tolerance of total energy, max ionic force, max ionic displacement, and max stress are set as  $5 \times 10^{-6} \, \text{eV} \, \text{atom}^{-1}$ ,  $2 \times 10^{-2} \, \text{eV} \, \text{Å}^{-1}$ ,  $5 \times 10^{-4} \, \text{Å}$  and  $2 \times 10^{-2} \, \text{GPa}$ , respectively. The generalized gradient approximation (GGA) $^{[41]}$  with Perdew–Burke–Ernzerhof (PBE) $^{[42]}$  functional was adopted. The norm-conserving pseudopotentials $^{[43-45]}$  are used, and the valence electrons of these elements are set as K:3s<sup>2</sup>3p<sup>6</sup>4s<sup>1</sup>, Rb:4s<sup>2</sup>4p<sup>6</sup>5s<sup>1</sup>, Cs:5s<sup>2</sup>5p<sup>6</sup>6s<sup>1</sup>, Sb:5s<sup>2</sup>5p<sup>3</sup>, F:2s<sup>2</sup>2p<sup>5</sup>, Cl:3s<sup>2</sup>3p<sup>5</sup>,

Br: $^4\text{s}^2\text{4p}^5$  I: $^5\text{s}^2\text{5p}^5$ . The cutoff energies were set as 940 eV for ASbF<sub>3</sub>Cl (A = K, Rb, Cs), and 830 eV for SbX<sub>3</sub> (X = Cl, Br, I). The Monkhorst–Pack k-point meshes, [46] spanning with less than 0.04 Å<sup>-3</sup> separation, were applied. The stability of these compounds was further confirmed by the phonon dispersion curves without any imaginary phonon model (shown in Figure 2 and S2, Supporting Information). The refractive indices and the bire-fringence were further calculated via the OptaDOS code. [47,48] To analyze the contribution of the anionic group to the nth-order susceptibility  $\chi(n)$ , a RSAC technique was adopted. [49,50] The projected band structures were also calculated using HSE06 functional [51–53] implemented in the PWMAT code. [54,55]

#### 3. Results and Discussion

# 3.1. The Structure of $ASbF_3Cl$ (A = K, Rb, Cs) and $SbX_3$ (X = Cl, Br, I)

Before deeply comprehending the electronic structures and optical properties, the authors would review their geometries first. The crystal structures of  $ASbF_3Cl$  (A = K, Rb, Cs) and  $SbX_3$  (X = Cl, Br, I) compounds are shown in **Figure 1** and S1, Supporting Information. As shown in Figure 1,  $KSbF_3Cl$  is isostructural with  $RbSbF_3Cl$ , and they all crystallize in the centrosymmetric (CS) orthorhombic space group Pbca (No. 61). Unlike  $ASbF_3Cl$  (A = K, Rb), the  $CsSbF_3Cl$  crystallizes in the noncentrosymmetric (NCS) tetragonal space group  $I\overline{4}2m$ . Noting that, the distorted antimony-centered polyhedra were found in these compounds which may have a relation with the asymmetric lone-pair electron distribution and may give a contribution to total optical properties. The distortion indices of different polyhedra



15213951, 2022, 7, Downloaded from https://onlinelibrary.wiley.com/doi/10.1002/pssb.202100576 by National Taiwan Universitaet, Wiley Online Library on [19/07/2023]. See the Terms

and-conditions) on Wiley Online Library for rules of use; OA articles are governed by the applicable Creative Commons License

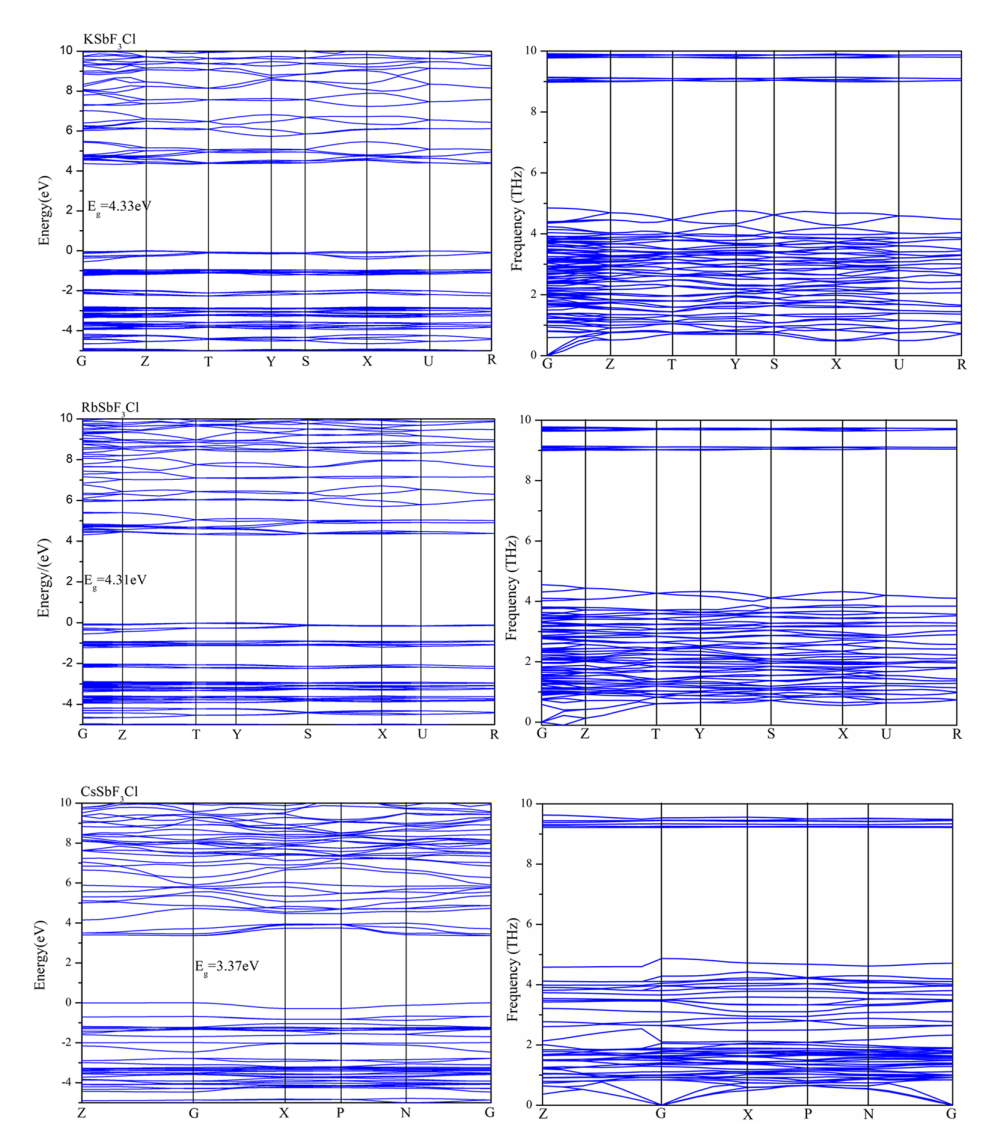


Figure 2. The band structure and phonon spectra of  $ASbF_3CI$  (A = K, Rb, and Cs).

are also calculated using Baur's method<sup>[56]</sup> implemented in the VESTA code<sup>[57]</sup> The obtained distortion degree of the tetrahedron SbF<sub>3</sub> in ASbF<sub>3</sub>Cl (A = K, Rb, Cs) is 0.00486, 0.00263, and 0.00663, respectively. However, the degree of tetrahedral distortion is not consistent with the birefringence trend (discussed in the following). The author believes that the tetrahedron in the system is not the main reason for the large birefringence.

SbCl<sub>3</sub> and SbBr<sub>3</sub> crystallized in the *Pbnm* space group. A virtual compound SbI<sub>3</sub> was obtained by replacing the Cl atom in SbCl<sub>3</sub> in the *Pbnm* space group with the I atom because there is still no experimental structure of SbI<sub>3</sub> reported. Like ASbF<sub>3</sub>Cl, the degree of distortion owns the sequence like SbBr<sub>3</sub> (0.00946) > SbCl<sub>3</sub> (0.00526) > SbI<sub>3</sub> (0.00396), which is different from the calculated birefringence SbI<sub>3</sub> (0.28) > SbBr<sub>3</sub> (0.22) > SbCl<sub>3</sub> (0.20). Hence, the authors would pay more attention to the role played by the antimony-centered polyhedra.

## 3.2. The Electronic Structures of ASbF3Cl (A = K, Rb, Cs) and SbX3 (X = Cl, Br, I)

Based on the aforementioned method, the electronic structure, phonon dispersion, and optical properties of  $ASbF_3Cl$  (A = K, Rb, Cs) and  $SbX_3$  (X = Cl, Br, I) are discussed. The band structure diagram and phonon spectrum diagram of those compounds are shown in Figure 2 and S2, Supporting Information. As shown in Figure 2, The  $KSbF_3Cl$ ,  $RbSbF_3Cl$ ,  $CsSbF_3Cl$  are indirect transition semiconductor, whose GGA-PBE gaps are 4.33, 4.31, 3.37 eV, respectively (shown in Table 1). The calculated bandgaps of  $RbSbF_3Cl$  and  $CsSbF_3Cl$  are comparable to those reported by Gong et al. [36] In addition, the absence of imaginary frequencies in the phonon spectrum proves that the structure is stable and can be used for further applications.

15213951, 2022, 7, Downloaded from https://onlinelibrary.wiley.com/doi/10.1002/pssb.202100576 by National Taiwan Universitaet, Wiley Online Library on [19/07/2023]. See the Terms and Conditional Con

on Wiley Online Library for rules of use; OA articles are governed by the applicable Creative Commons

**Table 1.** Space groups, calculated bandgaps with GGA/PBE functional and the Birefringence ( $\Delta n$ ) at 1064 nm.

Crystal	Space group	$E_{\rm g}$ [eV] (PBE)	Birefringence (@1064 nm)
KSbF₃Cl	Pbca	4.33	0.080
RbSbF <sub>3</sub> Cl	Pbca	4.31	0.061
CsSbF <sub>3</sub> Cl	R <del>4</del> 2/m	3.37	0.271
SbCl <sub>3</sub>	Pbnm	3.31	0.20
$SbBr_3$	Pbnm	2.92	0.22
SbI <sub>3</sub> **a)	Pbnm	2.80	0.28

<sup>&</sup>lt;sup>a)</sup>Sbl<sub>3</sub>\*\* was obtained by replacing the Cl atom in SbCl<sub>3</sub> with an I atom.

#### 3.3. The Lone Pair Electrons of ASbF<sub>3</sub>Cl (A = K, Rb, Cs)

It is well known that ELF and orbitals near the Fermi level are useful methods to describe localized electronic distribution like asymmetric lone-pair electronic distribution.<sup>[58]</sup> Hence the ELF was firstly calculated using the CASTEP package to distinguish the lone-pair electrons around Sb atoms. As shown in **Figure 3**, the crescent-like electronic distribution is found around Sb<sup>3+</sup>, indicating the stereochemically active lone pair electrons of Sb cations. Orbitals near the Fermi level (shown in Figure S3, Supporting Information) show similar results. In a word, the

asymmetric lone-pair electronic distribution is found around Sb<sup>3+</sup> cations, hence the authors want to dig out the atomic contribution to the total birefringence.

#### 3.4. The Atomic Contribution of Optical Properties

Using OptaDOS code, the birefringence of  $ASbF_3Cl$  (A = K, Rb, Cs) are obtained as 0.080, 0.061, and 0.271 @1064 nm, respectively. The birefringence diagram of ASbF<sub>3</sub>Cl (A = K, Rb, Cs) is shown in Figure 4. CsSbF<sub>3</sub>Cl has a considerably large birefringence comparison with other compounds. To further investigate the atomic/anionic group's contribution, RSAC method was used. In RSAC operation, the cutting radius follows the basic principle of keeping the atomic spheres in contact with each other without overlapping. For  $ASbF_3Cl$  (A = K, Rb, and Cs), the cutting radius are set as follows: 1.40 Å (K), 1.48 Å (Rb), 1.69 Å (Cs), 1.20 Å (Sb), 1.20 Å (F), and 1.50 Å (Cl). According to the atomic coordination environment, the threshold of chemical bond was set as 3.5 Å. The obtained refractive indices of groups are shown in Table 2. As shown in Table 2, the birefringence of [SbF<sub>3</sub>Cl<sub>2</sub>] group is even larger than the total birefringence of  $ASbF_3Cl$  (A = K, Rb, and Cs) compounds, implying the alkali metals may give a little contribution to the total birefringence. Further analysis of the interband transitions of atoms reveals that the [SbF<sub>3</sub>Cl<sub>2</sub>] group at the top of the valence band plays a decisive role in the birefringence of the material.

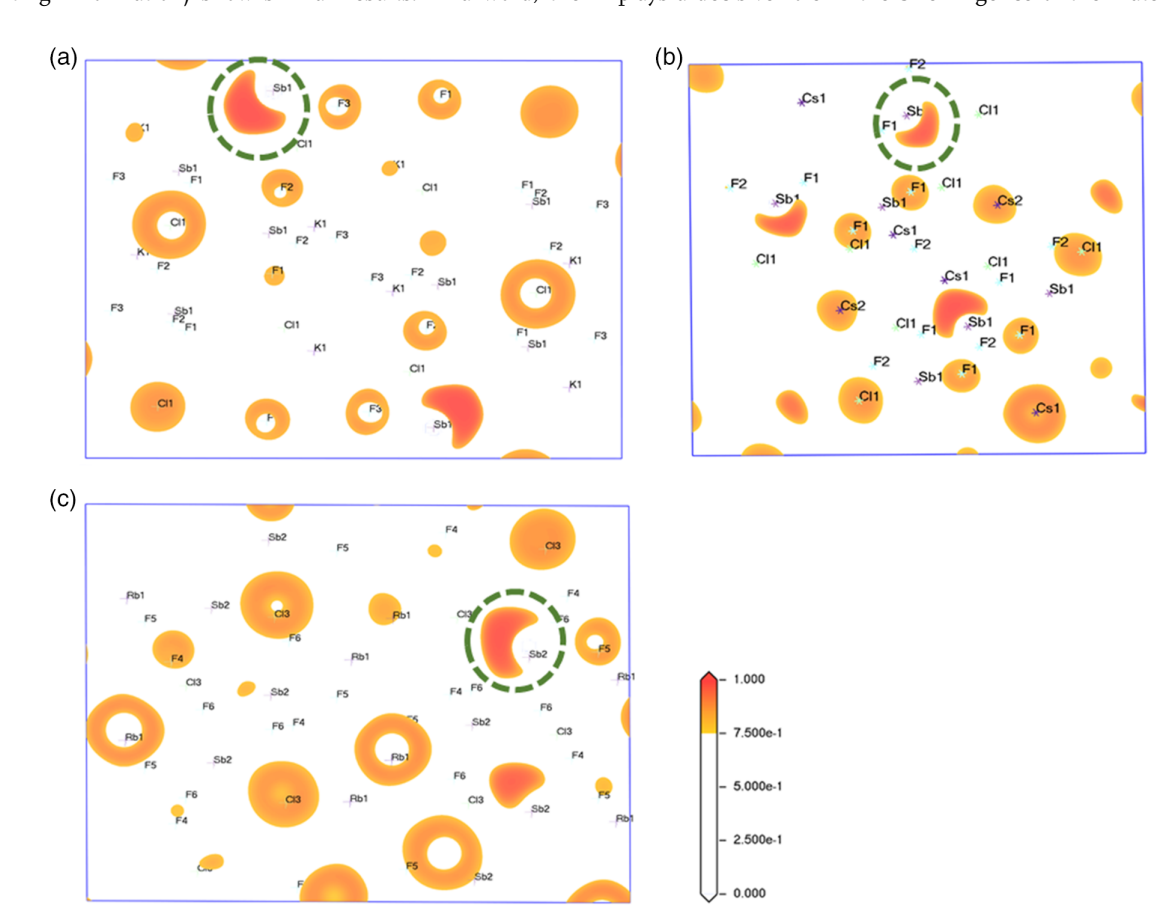


Figure 3. Election localization function (ELF) diagrams of: a) KSbF<sub>3</sub>Cl, b) RbSbF<sub>3</sub>Cl, and c) CsSbF<sub>3</sub>Cl.

1100

1200

1300

15213951, 2022, 7, Downloaded from https://onlinelibrary.wiley.com/doi/10.1002/pssb.202100576 by National Taiwan Universitaet, Wiley Online Library on [19/07/2023]. See the Terms

onditions) on Wiley Online Library for rules of use; OA articles are governed by the applicable Creative Commons

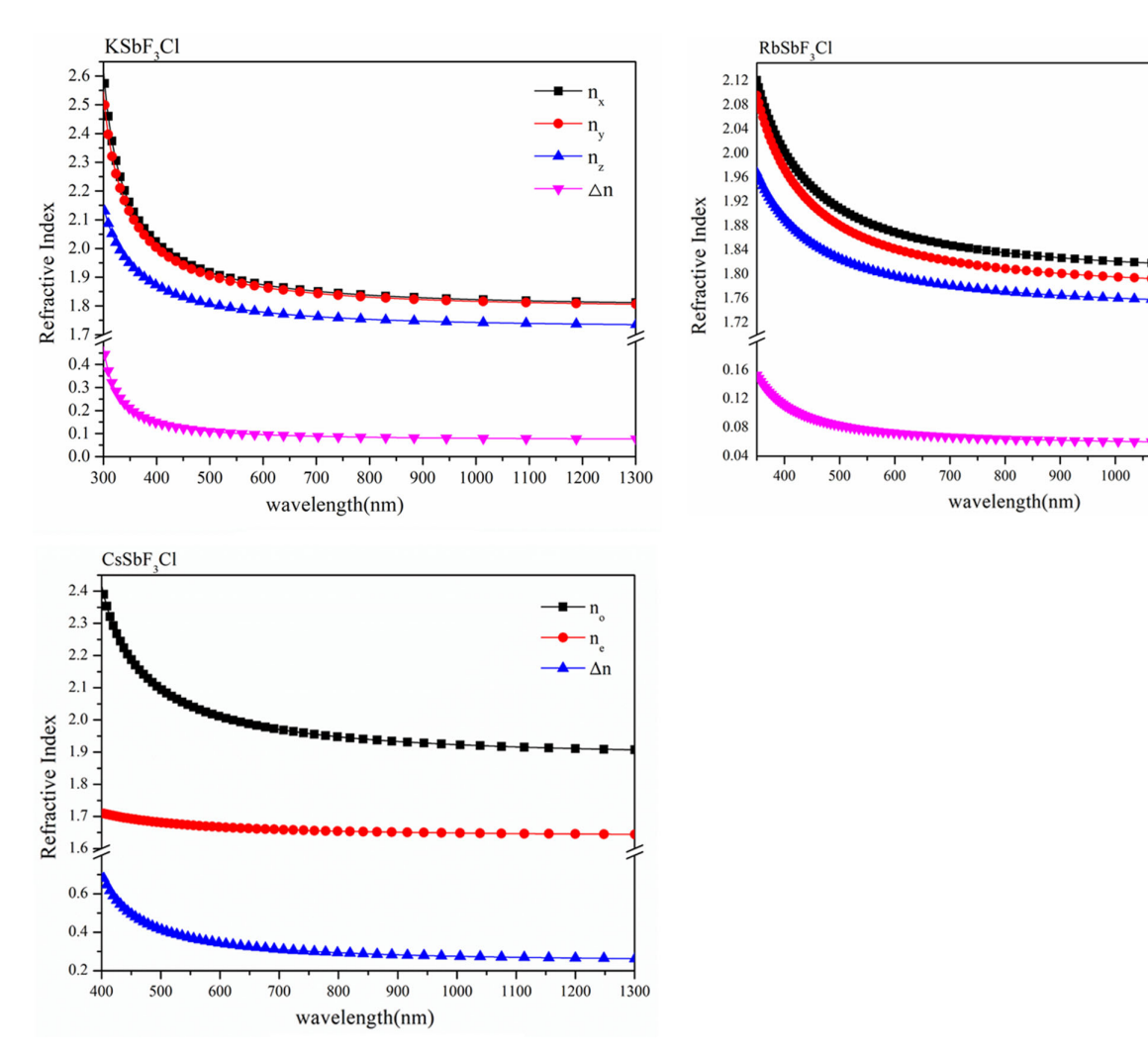


**Figure 4.** The birefringence of  $ASbF_3CI$  (A = K, Rb, and Cs).

To further dig out the atomic contribution from cations and halogens, the Born effective charges<sup>[59–61]</sup> of ASbF<sub>3</sub>Cl (A = K, Rb, Cs) were also calculated using the CASTEP code (shown in Table 3). As shown in Table 3, the alkali atoms (K, Rb, and Cs) give a relatively small contribution to the total birefringence due to their relatively small  $\Delta q$  values. For F atoms, they give both positive and negative contributions to anisotropic optical birefringence. Unlike F atoms, the Cl atoms give a positive contribution to birefringence due to their positive  $\Delta q$  values. The largest  $\Delta q$  values are found in Sb atoms indicating the lone-pair electronic distribution gives the main contribution to the total birefringence.

It is well known that the optical properties are determined by the electron transition from the states at the top of the valence band to the bottom of the conduction band. The obtained projected density of states (PDOS) of ASbF<sub>3</sub>Cl (A = K, Rb, Cs) is also shown in Figure 5. To better describe the interaction among these atoms, the states at the top of the valence band are divided into three different energy regions (shown in Figure 5). Based on the PDOS, several observations can be obtained as follows:

1) For  $ASbF_3Cl$  (A = K, Rb, Cs), hardly any electrons from alkali metal atoms can be found at the top of the valence band, implying the alkali atoms may give a little contribution to the optical properties, which is in good agreement with the conclusions obtained by RSAC and Born effective charge. 2) It is worth noting that the F-p is mainly concentrated in the II region far away from the Fermi level, while the Cl-p state is in the III region, which is closer to the Fermi level. 3) In the I region, the top of the valence band near the Fermi surface and the bottom of the conduction band far from the Fermi surface is mainly composed of Sb-sp orbitals containing lone pairs of electrons, Cl-p orbitals, and Sb-p orbitals. To visually see the contribution of each element, the projected band structures calculated using PWMAT code are also obtained. As shown in Figure S4-S6, Supporting Information, it can be clearly seen that the Cl-p orbitals appear near the Fermi level, while the F-p orbitals appear at  $-5 \approx -2$  eV for the  $ASbF_3Cl$  (A = K, Rb, Cs). Similarly, in the projected band structures, the orbits near the Fermi surface are mainly composed of Sb-sp and Cl-p orbitals. Therefore, we believe that the larger birefringence of the system is mainly derived from

1521391, 2022, 7, Downloaded from https://onlinelibrary.wiley.com/doi/10.1002/pssb.202100576 by National Taiwan Universitat, Wiley Online Library on [1907/2023], See the Terms and Conditions (https://onlinelibrary.wiley.com/terms-and-conditions) on Wiley Online Library for rules of use; OA articles are governed by the applicable Creative Commons Licrossystems (https://onlinelibrary.wiley.com/terms-and-conditions) on Wiley Online Library for rules of use; OA articles are governed by the applicable Creative Commons Licrossystems (https://onlinelibrary.wiley.com/terms-and-conditions) on Wiley Online Library for rules of use; OA articles are governed by the applicable Creative Commons Licrossystems (https://onlinelibrary.wiley.com/terms-and-conditions) on Wiley Online Library for rules of use; OA articles are governed by the applicable Creative Commons Licrossystems (https://onlinelibrary.wiley.com/terms-and-conditions) on Wiley Online Library for rules of use; OA articles are governed by the applicable Creative Commons Licrossystems (https://onlinelibrary.wiley.com/terms-and-conditions) on Wiley Online Library for rules of use; OA articles are governed by the applicable Creative Commons Licrossystems (https://onlinelibrary.wiley.com/terms-and-conditions) on Wiley Online Library for rules of use; OA articles are governed by the applicable Creative Commons (https://onlinelibrary.wiley.com/terms-and-conditions) on the applicable Creative Commons (https://onlinelibrary.wiley.com/terms-and



**Table 2.** The refractive indices and birefringence of different anionic groups in  $ASbF_3CI$  (a = K, Rb, and Cs) obtained by the RSAC method.

Crystal	Valence Bands	Conduction Bands	n <sub>x</sub>	nγ	nz	$\Delta n$
KSbF₃Cl	Origin		1.714	1.709	1.634	0.080
	K	K	1.080	1.079	1.071	0.009
	$SbF_3Cl_2$	SbF <sub>3</sub> Cl <sub>2</sub>	1.705	1.700	1.624	0.081
	K, SbF <sub>3</sub> Cl <sub>2</sub>	K	1.714	1.709	1.634	0.080
	K, SbF <sub>3</sub> Cl <sub>2</sub>	SbF <sub>3</sub> Cl <sub>2</sub>	1.714	1.709	1.634	0.080
	K	K, SbF <sub>3</sub> Cl <sub>2</sub>	1.041	1.040	1.039	0.002
	$SbF_3Cl_2$	K, SbF <sub>3</sub> Cl <sub>2</sub>	1.700	1.707	1.631	0.080
RbSbF <sub>3</sub> Cl	C	Drigin	1.693	1.667	1.632	0.061
	Rb	Rb	1.093	1.091	1.081	0.012
	SbF <sub>3</sub> Cl <sub>2</sub>	$SbF_3Cl_2$	1.675	1.647	1.612	0.063
	Rb, SbF <sub>3</sub> Cl <sub>2</sub>	Rb	1.693	1.667	1.632	0.061
	Rb, SbF <sub>3</sub> Cl <sub>2</sub>	SbF <sub>3</sub> Cl <sub>2</sub>	1.693	1.667	1.632	0.061
	Rb	Rb, SbF <sub>3</sub> Cl <sub>2</sub>	1.050	1.049	1.049	0.001
	$SbF_3Cl_2$	Rb, SbF <sub>3</sub> Cl <sub>2</sub>	1.679	1.651	1.616	0.063
CsSbF₃Cl	C	Drigin	1.918	1.918	1.647	0.271
	Cs	Cs	1.274	1.274	1.233	0.040
	$SbF_3Cl_2$	SbF <sub>3</sub> Cl <sub>2</sub>	1.810	1.810	1.513	0.294
	Cs, SbF <sub>3</sub> Cl <sub>2</sub>	Cs	1.913	1.913	1.647	0.265
	Cs, SbF <sub>3</sub> Cl <sub>2</sub>	SbF <sub>3</sub> Cl <sub>2</sub>	1.913	1.913	1.647	0.265
	Cs	Cs, SbF <sub>3</sub> Cl <sub>2</sub>	1.237	1.237	1.223	0.014
	SbF <sub>3</sub> Cl <sub>2</sub>	Cs, SbF <sub>3</sub> Cl <sub>2</sub>	1.813	1.813	1.521	0.292

**Table 3.** The obtained Born effective charges in  $ASbF_3CI$  (A = K, Rb, and Cs).

	Atom	$q_{xx}$	$q_{\gamma\gamma}$	$q_{zz}$	Δq
KSbF <sub>3</sub> Cl	K	1.17627	1.27766	1.21167	-0.10139
	Sb	3.03605	2.58009	2.87252	0.45596
	F(1,4,7,10,13,16,19,22)	-0.63407	-0.55048	-1.56769	0.08359
	F(2,5,8,11,14,17,20,23)	-1.57881	-0.51496	-0.64676	1.06385
	F(3,6,9,12,15,18,21,24)	-0.65121	-1.56843	-0.57792	-0.91722
	Cl	-1.34822	-1.22388	-1.29182	0.12434
RbSbF <sub>3</sub> Cl	Rb	1.26598	1.24389	1.33258	-0.0666
	Sb	2.93741	2.90763	2.63262	0.30479
	F(1,4,7,10,13,16,19,22)	-1.59234	-0.62599	-0.5619	1.03044
	F(2,5,8,11,14,17,20,23)	-0.56826	-0.64868	-1.60636	-1.0381
	F(3,6,9,12,15,18,21,24)	-0.67692	-1.52984	-0.52964	0.14728
	Cl	-1.36587	-1.34701	-1.26731	0.09856
CsSbF <sub>3</sub> Cl	Cs(1,2)	1.30426	1.30426	1.26849	0.03577
	Cs(3,4)	1.17906	1.17906	1.55187	-0.37281
	Sb	3.26683	3.26683	2.32761	0.93922
	F(1,2,5,6)	-1.63473	-0.53316	-0.87809	-0.34493
	F(3,4,7,8)	-0.53316	-1.63473	-0.87809	0.75664
	F(9,10,11,12)	-0.80753	-0.80753	-1.00838	-0.20085
	CI(1,2)	-0.97471	-2.09141	-0.97322	1.11819
	Cl(3,4)	-2.09141	-0.97471	-0.97322	0.00149

the Cl element and the cation Sb containing a lone pair of electrons.

To further study the different contributions of the F and Cl elements, two virtual compounds CsSbF4 and CsSbCl4 are obtained using atom-substitution from CsSbF<sub>3</sub>Cl. The bandgap of CsSbF<sub>4</sub> and CsSbCl<sub>4</sub> are 3.69 and 3.15 eV. The birefringence of CsSbF4 and CsSbCl4 is 0.124 and 0.210, respectively. The birefringence of CsSbCl4 was significantly larger than the birefringence of CsSbF<sub>4</sub>, implying the Cl atoms are beneficial to enlarge birefringence comparison with F atoms. The obtained PDOS of CsSbF4 and CsSbCl4 are also shown in Figure S6, Supporting Information. The peak position of the F-p state in the PDOS of CsSbF<sub>4</sub> is about -3 to -2 eV, which is far away from the Fermi level. In contrast, the peak position of the Cl-p state in the PDOS of CsSbCl₄ is between −1 and 0 eV nearby the Fermi level, implying Cl atoms play an important role in obtaining enhanced birefringence, and the states nearby the Fermi level give the main contribution to the birefringence.

#### 3.5. The Optical Properties of Binary $SbX_3$ (X = Cl, Br, I)

To deeply understand the atomic contribution from antimony and halogens, the authors also calculated the electronic structures and birefringence of binary compounds without alkali atoms. Bandgap, birefringence, and other data of  $SbX_3$  ( $X=Cl,\ Br,\ I$ ) halides are shown in Table 1. As shown in Table 1, like  $ASbF_3Cl$  ( $A=K,\ Rb,\ Cs$ ) compounds, the bandgap of these binary compounds decreased from Cl to I, and the birefringence increased from Cl to I. Therefore, the author believes that the birefringence of the compound is related to the distribution of electronic states near the Fermi surface. The PDOS of  $SbX_3$  ( $X=Cl,\ Br,\ I$ ) are also obtained (shown in Figure 6). As shown in Figure 6, the interaction between Sb-sp states and halogens' p states are found at the top of the valence band. And the authors also found out that from Cl to I, the peak of halogens is gradually closer to the Fermi surface.

Like ASbF<sub>3</sub>Cl (A = K, Rb, Cs), the SbX<sub>3</sub> (X = Cl, Br, I) system also has stereochemically active lone pairs, which were characterized by orbitals near the Fermi level and ELF. The orbit near the Fermi level is shown in **Figure 7**. The asymmetric density around Sb atoms, i.e., lone-pair electrons is observed. As shown in Figure 7, it can be clearly seen that the stereochemical activity of lone pair electrons of antimony atom is  $SbCl_3 > SbBr_3 > SbI_3$ , although the birefringence of the  $SbX_3$  (X = Cl, Br, I) system is  $SbCl_3 < SbBr_3 < SbI_3$ . ELF shows the same result, as shown in Figure S8, Supporting Information. Based on the earlier discussion, the author will further study the contribution of Sb atoms containing lone pairs of electrons to the birefringence of compounds.

#### 3.6. The Atomic Contribution to Lone-Pairs and Birefringence

The mechanism of stereochemical active lone-pair has long been a hot issue.<sup>[62–65]</sup> The stereochemical activity of ns<sup>2</sup> lone pairs was determined by the hybridization of states. The revised model suggested by Walsh et al.<sup>[66]</sup> mentioned on the isolated atomic energy level that relative energy of the X-s and Y-p states (X is cationic atom like Pb, Sn, Sb, Bi; Y is anionic atom like O) is

15213951, 2022, 7, Downloaded from https://onlinelibrary.wiley.com/doi/10.1002/pssb.202100576 by National Taiwan Universitaet, Wiley Online Library on [19/07/2023]. See the Terms

conditions) on Wiley Online Library for rules of use; OA articles are governed by the applicable Creative Commons License

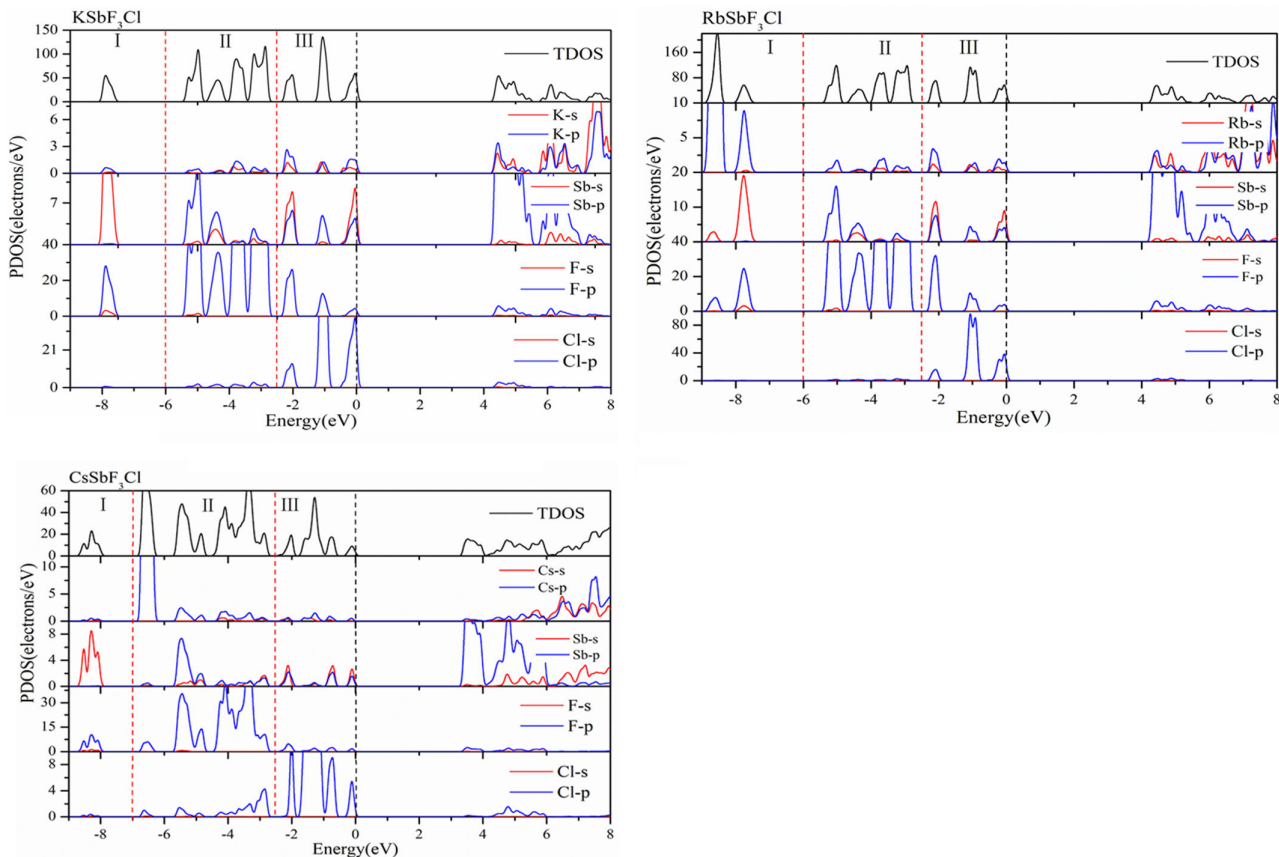


Figure 5. The projected density of states (PDOS) of  $ASbF_3Cl$  (A = K, Rb, and Cs).

critical to the formation of stereochemically active lone-pair electrons in the metal oxides. The closer between two atoms are in energy, the stronger interaction and the more cation states are present in the upper valence band, leading to more stereochemically activity of lone pairs. In this article, the atomic energies of antimony and halogens are recalculated using the Gaussian09 code. [67] Based on the density functional theory, the LanL2DZ basis set [68–70] is used to calculate the orbital energy. As shown in **Figure 8**, the energy difference between the s-state of the cation and the *p*-state of the halogen own the sequence as Sb-Cl < Sb-Br < Sb-I, consistent with the stereochemical activity of Sb (III) cations found in ternary and binary post-transition metal halides described earlier. Hence, the authors believe that the revised model about lone-pairs can also be suitable in post-transition metal halides.

Let us turn back to the PDOS of bulk  $SbX_3$  compounds. As for the source of the contribution to the optical properties, we know that it is related to the electron transitions near the Fermi surface. In the PDOS diagram, we find that there are relatively more Sb-p orbitals at the top of the valence band and at the bottom of the conduction band. Therefore, it is suggested that the p-orbitals of cations play an important role in determining birefringence. To further verify the contribution of cation p-orbitals, R(Sb-p) is used to describe quantitatively. The ratio is defined as

$$R(Sb-p) = S(Sb-p)/(S(Sb-s) + S(Sb-p) + S(X-p))$$
 (1)

where R(Sb-p) is the ratio of Sb p states to Sb p (Sb s–X p) \* states, and the S(Sb-s), S(Sb-p) and S(X-p) are the intensities of Sb-s states, Sb-p states, and X-p states, respectively. The obtained ratio of Sb-p was shown in **Table 4**. As shown in Table 4, R(Sb-p) owns the sequence as  $SbCl_3$  (0.094) <  $SbBr_3$  (0.11) <  $SbI_3$  (0.12), consistent well with the trend found in birefringence, indicating the Sb-p states play an important role in determining the birefringence.

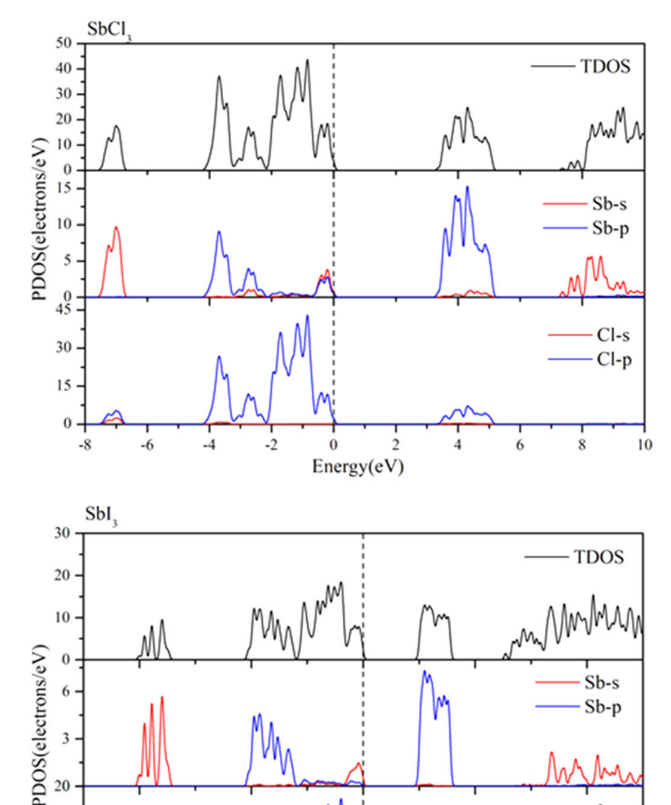
### 4. Conclusion

In this article, the electronic structures and birefringence of post-transition metal halides  $ASbF_3Cl$  (A=K, Rb, Cs) and  $SbX_3$  (X=Cl, Br, I) were investigated using the first-principles method. Some conclusions are listed as follows: 1) The asymmetric lone-pair electronic distribution is found around the antimony cations, and the stereochemical activity of antimony cations in these compounds gradually decreased from Cl to I. The degree of stereochemical activity of lone pairs is determined by the energy difference between the s-state of the cation and the p-state of the halogen, implying the revised model about the stereochemical activity of lone pairs in metal oxides is also appropriate for metal halides. 2) The birefringence of these

10

15213951, 2022, 7, Downloaded from https://onlinelibrary.wiley.com/doi/10.1002/pssb.202100576 by National Taiwan Universitaet, Wiley Online Library on [19/07/2023]. See the Terms and Condition of the Conditional Taiwan Universitated and Conditional Taiwan Universitated

onditions) on Wiley Online Library for rules of use; OA articles are governed by the applicable Creative Commons License



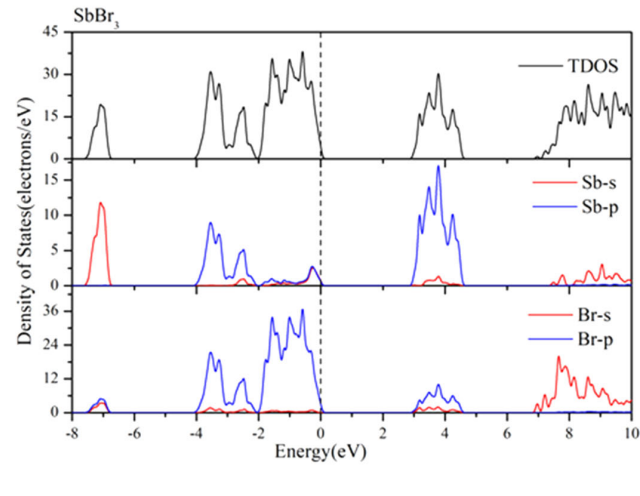
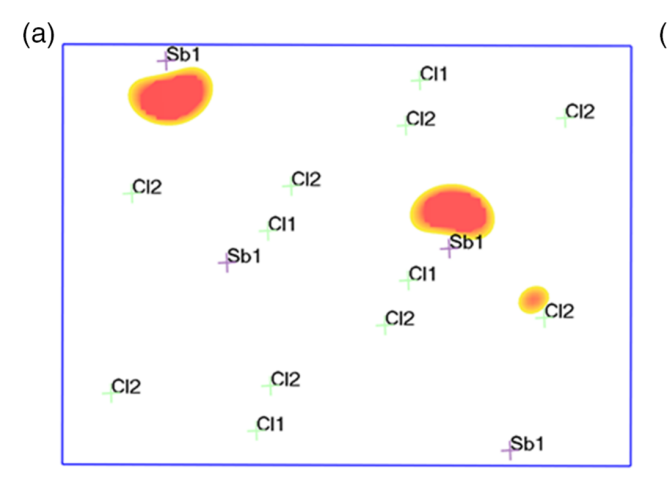


Figure 6. The projected density of states (PDOS) of  $SbX_3(X = CI, Br, I)$ .

compounds gradually increased from Cl to I. The real-space atomic cutting and Born effective charges show that the antimony cations and halogen closer to Fermi level give the main contribution to birefringence. And the occupied p states of antimony and halogen atoms play an important role in

determining the birefringence which can be confirmed by the ratio of p-states. The obtained conclusions can help to design and synthesize novel nonlinear optical materials, photovoltaic materials, and antimony halide compounds with excellent optical properties.



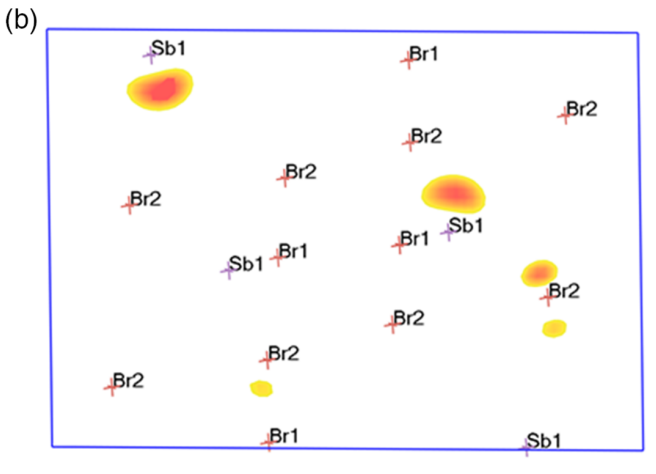


Figure 7. The  $SbX_3(X = Cl, Br, I)$  electron density map of orbital nearing Fermi level.

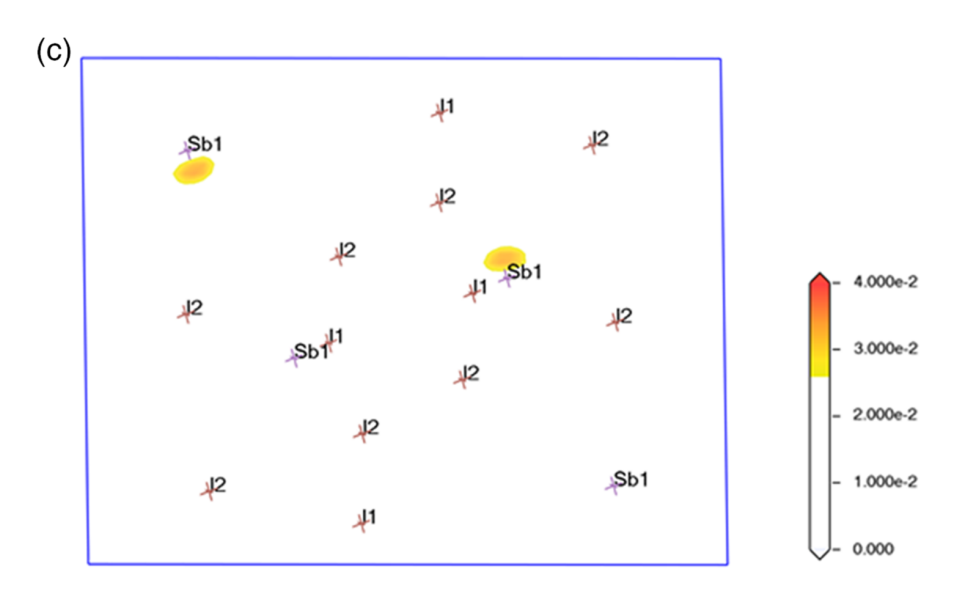
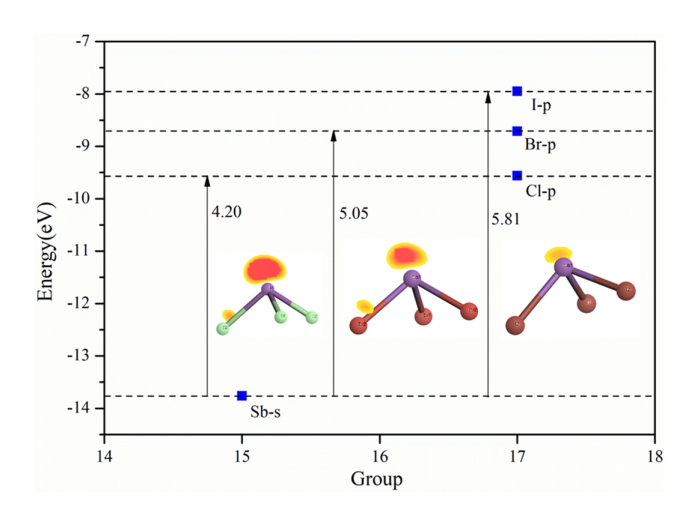


Figure 7. Continued.



**Figure 8.** The orbital energy and their difference of antimony and halogen atoms obtained by Gaussian code.

**Table 4.** The optical properties and PDOS integral area of  $SbX_3$  (X = Cl, Br, I).

SbX <sub>3</sub>	Δn (@1064 nm)	PDOS integral area			
		Sb-s	Sb-p	Х-р	R(Sb-p)
SbCl <sub>3</sub>	0.20	6.66	7.34	64.11	0.094
$SbBr_3$	0.22	6.44	8.46	63.00	0.11
Sbl <sub>3</sub> **	0.28	5.46	9.47	61.83	0.12

#### **Supporting Information**

Supporting Information is available from the Wiley Online Library or from the author.

## Acknowledgements

L.L. and Y.Q. contributed equally to this work. This work is supported by the National Natural Science Foundation of China (Grant No. 11864040), the Natural Science Foundation of Xinjiang Uygur Autonomous Region of China (Grant No. 2018D01C072), the National Undergraduate Training Program for Innovation (Grant No. S202010755088), and Tianshan Innovation Team Program of Xinjiang Uygur Autonomous Region (Grant No. 2020D14038).

#### **Conflict of Interest**

The authors declare no conflict of interest.

#### **Data Availability Statement**

The data that support the findings of this study are available from the corresponding author upon reasonable request.

#### **Keywords**

antimony, birefringence, metal halides, stereochemical activity

Received: November 9, 2021 Revised: February 28, 2022 Published online: March 20, 2022

- [1] Y. Xia, C. Chen, D. Tang, B. Wu, Adv. Mater. 1995, 7, 79.
- [2] P. Bordui, M. Fejer, Annu. Rev. Mater. Res. 2003, 23, 321.
- [3] J. Wang, H. Yu, Y. Wu, R. Boughton, Engineering 2015, 1, 192.
- [4] H. Wu, H. Yu, Z. Yang, X. Hou, X. Su, S. Pan, K. R. Poeppelmeier, J. M. Rondinelli, J. Am. Chem. Soc. 2013, 135, 4215.
- [5] G. Q. Shi, Y. Wang, F. F. Zhan, B. B. Zhang, R. H. Yang, X. L. Hou, S. L. Pan, K. R. Poeppelmeier, J. Am. Chem. Soc. 2017, 139, 10645.
- [6] B. Zhang, G. Shi, Z. Yang, F. Zhang, S. Pan, Angew. Chem. Int. Ed. 2017, 56, 3916.



- [7] X. Wang, Y. Wang, B. Zhang, F. Zhang, Z. Yang, S. Pan, Angew. Chem. Int. Ed. 2017, 56, 14119.
- [8] J. Chen, L. Xiong, L. Chen, L. M. Wu, J. Am. Chem. Soc. 2018, 140, 14082
- [9] M. Mutailipu, M. Zhang, Z. H. Yang, S. L. Pan, Acc. Chem. Res. 2019, 52, 791.
- [10] M. Mutailipu, S. Pan, Angew. Chem. Int. Ed. 2020, 59, 20302.
- [11] Z. Jin, Z. Zhang, J. Xiu, H. Song, T. Gatti, Z. He, J. Mater. Chem. A 2020, 8, 16166.
- [12] C. Chen, B. Wu, A. Jiang, G. You, Sci. Sin. B 1985, 28, 235.
- [13] C. Chen, Y. Wu, A. Jiang, B. Wu, G. You, R. Li, S. Lin, J. Opt. Soc. Am. B 1989, 6, 616.
- [14] Y. Wu, T. Sasaki, S. Nakai, A. Yokotani, H. Tang, C. Chen, Appl. Phys. Lett. 1993, 62, 2614.
- [15] L. Mei, X. Huang, Y. Wang, Q. Wu, B. Wu, C. Chen, Z. Kristallogr. 1995, 210, 93.
- [16] C. Chen, Z. Xu, D. Deng, J. Zhang, G. K. L. Wong, B. Wu, N. Ye, D. Tang, Appl. Phys. Lett. 1996, 68, 2930.
- [17] M. Mutailipu, M. Zhang, Z. Yang, S. Pan, Acc. Chem. Res. 2019, 52, 791
- [18] H. Wu, S. Pan, K. R. Poeppelmeier, H. Li, D. Jia, Z. Chen, X. Fan, Y. Yang, J. M. Rondinelli, H. Luo, J. Am. Chem. Soc. 2011, 133, 7786.
- [19] M. Mutailipu, M. Zhang, H. Wu, Z. Yang, Y. Shen, J. Sun, S. Pan, Nat. Commun. 2018, 9, 3089.
- [20] Y. Wang, B. Zhang, Z. Yang, S. Pan, Angew. Chem. Int. Ed. 2018, 57, 2150
- [21] X. Chen, B. Zhang, F. Zhang, Y. Wang, M. Zhang, Z. Yang, K. R. Poeppelmeier, S. Pan, J. Am. Chem. Soc. 2018, 140, 16311.
- [22] G. Peng, N. Ye, Z. Lin, L. Kang, S. Pan, M. Zhang, C. Lin, X. Long, M. Luo, Y. Chen, Y. H. Tang, F. Xu, T. Yan, Angew. Chem. Int. Ed. Engl. 2018, 57, 8968.
- [23] S. Wang, N. Ye, W. Li, D. Zhao, J. Am. Chem. Soc. 2010, 132, 8779.
- [24] S. Zhao, X. Yang, Y. Yang, X. Kuang, F. Lu, P. Shan, Z. Sun, Z. Lin, M. Hong, J. Luo, J. Am. Chem. Soc. 2018, 140, 1592.
- [25] S. Liu, X. Liu, S. Zhao, Y. Liu, L. Li, Q. Ding, Y. Li, Z. Lin, J. Luo, M. Hong, Angew. Chem. Int. Ed. Engl. 2020, 59, 9414.
- [26] S. Han, M. Mutailipu, A. Tudi, Z. Yang, S. Pan, Chem. Mater. 2020, 32, 2172.
- [27] Q. Jing, X. Dong, X. Chen, Z. Yang, S. Pan, C. Lei, Chem. Phys. 2015, 453–454, 42.
- [28] Y. Liu, X. Liu, S. Liu, Q. Ding, Y. Li, L. Li, S. Zhao, Z. Lin, J. Luo, M. Hong, Angew. Chem. Int. Ed. 2020, 59, 7793.
- [29] E. N. Rao, G. Vaitheeswaran, A. H. Reshak, S. Auluck, RSC Adv. 2016, 6, 99885.
- [30] E. Narsimha Rao, G. Vaitheeswaran, A. H. Reshak, S. Auluck, Phys. Chem. Chem. Phys. 2017, 19, 31255.
- [31] E. Narsimha Rao, S. Appalakondaiah, N. Yedukondalu, G. Vaitheeswaran, J. Solid State Chem. 2014, 212, 171.
- [32] H. Zhang, M. Zhang, S. Pan, X. Dong, Z. Yang, X. Hou, Z. Wang, K. B. Chang, K. R. Poeppelmeier, J. Am. Chem. Soc. 2015, 137, 8360.
- [33] X. Chen, Q. Jing, K. M. Ok, Angew. Chem. Int. Ed. 2020, 59, 2033.
- [34] X. Chen, H. Jo, K. M. Ok, Angew. Chem. Int. Ed. Engl., 2020, 59, 7514.
- [35] J. Guo, A. Tudi, S. Han, Z. Yang, S. Pan, Angew. Chem. Int. Ed. 2020, 133, 3582
- [36] P. Gong, Y. Yang, F. You, X. Zhang, G. Song, S. Zhang, Q. Huang, Z. Lin, Cryst. Growth Des. 2019, 19, 1874.
- [37] S. J. Clark, M. D. Segall, C. J. Pickard, P. J. Hasnip, M. I. J. Probert, K. Refson, M. C. Payne, Z. Kristallogr.-Cryst. Mater. 2005, 220, 567.

- [38] V. Milman, K. Refson, S. J. Clark, C. J. Pickard, J. R. Yates, S. P. Gao, P. J. Hasnip, M. I. J. Probert, A. Perlov, M. D. Segall, J. Mol. Struct. Theochem. 2010, 954, 22.
- [39] D. Vanderbilt, Phys. Rev. B 1990, 41, 7892.
- [40] W. Kohn, Rev. Mod. Phys. 1999, 71, 1253.
- [41] D. M. Ceperley, B. J. Alder, Phys. Rev. Lett. 1980, 45, 566.
- [42] J. P. Perdew, K. Burke, M. Ernzerhof, Phys. Rev. Lett. 1996, 77, 3865.
- [43] L. Kleinman, D. Bylander, Phys. Rev. Lett. 1982, 48, 1425.
- [44] J. S. Lin, A. Qteish, M. C. Payne, V. V. Heine, Phys. Rev. B 1993, 47, 4174
- [45] D. R. Hamann, M. Schlüter, C. Chiang, Phys. Rev. Lett. 1979, 43, 1494.
- [46] H. J. Monkhorst, J. D. Pack, Phys. Rev. B 1976, 13, 5188.
- [47] R. J. Nicholls, A. J. Morris, C. J. Pickard, J. R. Yates, J. Phys. Conf. Ser. 2012, 371, 012062.
- [48] A. J. Morris, R. J. Nicholls, C. J. Pickard, J. R. Yates, Comput. Phys. Commun. 2014, 185, 1477.
- [49] Z. Lin, J. Lin, Z. Wang, C. Chen, M.-H. Lee, Phys. Rev. B 2000, 62, 1757.
- [50] J. Lin, M.-H. Lee, Z.-P. Liu, C. Chen, C. J. Pickard, Phys. Rev. B 1999, 60, 13380.
- [51] J. Paier, M. Marsman, K. Hummer, G. Kresse, I. C. Gerber, J. G. Ángyán, J. Chem. Phys. 2006, 125, 154709.
- [52] A. V. Krukau, O. A. Vydrov, A. F. Izmaylov, G. E. Scuseria, J. Chem. Phys. 2006, 125, 224106.
- [53] J. Heyd, G. E. Scuseria, J. Chem. Phys. 2004, 120, 7274.
- [54] W. Jia, J. Fu, Z. Cao, L. Wang, X. Chi, W. Gao, L.-W. Wang, J. Comput. Phys. 2013, 251, 102.
- [55] W. Jia, Z. Cao, L. Wang, J. Fu, X. Chi, W. Gao, L.-W. Wang, Comput. Phys. Commun. 2013, 184, 9.
- [56] K. Momma, F. Izumi, J. Appl. Crystallogr. 2011, 44, 1272.
- [57] H. Xiao, J. Tahir-Kheli, I. I. I. Goddard, J. Phys. Chem. Lett. 2011, 2, 212.
- [58] P. Politzer, J. S. Murray, J. Theor. Comput. Chem. 1996, 649.
- [59] R. Resta, D. Vanderbilt, Top. Appl. Phys. 2007, 105, 31.
- [60] N. A. Spaldin, J. Solid State Chem. 2012, 195, 2.
- [61] Q. Jing, G. Yang, J. Hou, M. Sun, H. Cao, J. Am. Chem. Soc. 2016, 244, 69.
- [62] P. Pyykko, Chem. Rev. 1988, 88, 563.
- [63] I. Lefebvre, M. Lannoo, G. Allan, A. Ibanez, J. Fourcade, J. C. Jumas, E. Beaurepaire, Phys. Rev. Lett. 1987, 59, 2471.
- [64] X. F. Hao, A. Stroppa, S. Picozzi, A. Filippetti, C. Franchini, Phys. Rev. B 2012, 86, 014116.
- [65] W.-P. Zhao, C. Shi, A. Stroppa, D. Di Sante, F. Cimpoesu, W. Zhang, Inorg. Chem. 2016, 55, 10337.
- [66] A. Walsh, D. J. Payne, R. G. Egdell, G. W. Watson, Chem. Soc. Rev. 2011, 40, 4455.
- [67] M. J. Frisch, G. W. Trucks, H. B. Schlegel, G. E. Scuseria, M. A. Robb, A. R. Cheeseman, G. Scalmani, V. Barone, B. Mennucci, G. A. Petersson, H. Nakatsuji, M. Caricato, X. Li, H. P. Hratchian, A. F. Izmaylov, J. Bloino, G. Zheng, J. L. Sonnenberg, M. Hada, M. Ehara, K. Toyota, R. Fukuda, J. Hasegawa, M. Ishida, T. Nakajima, Y. Honda, O. Kitao, H. Nakai, T. Vreven, J. A. Montgomery, et al., Gaussian 09, Rev. E.01, Gaussian, Inc., Wallingford CT 2013.
- [68] P. J. Hay, W. R. Wadt, J. Chem. Phys. 1985, 82, 270.
- [69] P. J. Hay, W. R. Wadt, J. Chem. Phys. 1985, 82, 299.
- [70] W. R. Wadt, P. J. Hay, J. Chem. Phys. 1985, 82, 284.